

5. MEASURED PERMEABILITIES OF DIATOMACEOUS SEDIMENTS AND PELAGIC CLAY FROM THE NORTHWEST PACIFIC, ODP SITE 1179¹

Ohmyoung Kwon,² Karen Mobley,² and Richard L. Carlson²

ABSTRACT

One of the objectives of drilling at Site 1179 was to search for microbes or biochemical evidence of microbial activity as part of the ongoing exploration of the depth and extent of the deep biosphere. The existence of living microbes has not been confirmed, but the chemistry of pore waters from the site, such as sulfate and ammonium profiles, is consistent with sulfate reduction and nitrification by anaerobic bacteria. However, chemical profiles are affected by the movement of molecules and ions through porous sediments by diffusion and advection. Permeability is thus an important consideration in the interpretation of pore water chemistry profiles. Moreover, diatomaceous sediments have some unique and, as yet, poorly understood physical properties. The purpose of this research is to measure hydraulic conductivity (permeability) in a suite of sediment samples from Ocean Drilling Program Site 1179 by the transient-pulse method. The sample set consists of four diatom ooze samples from Unit I, one radiolarian ooze sample from Unit II, and one pelagic clay sample from Unit III. The permeability of the clay is 1.92 μd , whereas the permeabilities of the overlying radiolarian and diatom oozes range from 289 to 1604 μd . Among these samples, permeability increases with porosity and grain size, in keeping with the results of previous studies.

¹Kwon, O., Mobley, K., and Carlson, R.L., 2004. Measured permeabilities of diatomaceous sediments and pelagic clay from the northwest Pacific, ODP Site 1179. In Sager, W.W., Kanazawa, T., and Escutia, C. (Eds.), *Proc. ODP, Sci. Results*, 191, 1–16 [Online]. Available from World Wide Web: <http://www-odp.tamu.edu/publications/191_SR/VOLUME/CHAPTERS/005.PDF>. [Cited YYYY-MM-DD]

²Department of Geology and Geophysics and Center for Tectonophysics, Texas A&M University, College Station TX 77845, USA. Correspondence author: carlson@geo.tamu.edu

Initial receipt: 6 January 2003
Acceptance: 29 March 2004
Web publication: 29 July 2004
Ms 191SR-005

BACKGROUND

Previous studies of permeability in deep-sea sediments have been motivated by efforts to understand the physical processes of compaction and fluid transport in deep-sea sediments. The objectives of a previous study by Bryant and Rack (1990), for example, were to determine the consolidation characteristics of the material and the affect of diatoms on the porosity and permeability of marine sediments. Many studies of permeability in deep-sea sediments have focused on environments where hydrologic processes are known to be active, along convergent margins such as Cascadia, Nankai, and Barbados (e.g., Moran and Christian, 1990; Taylor et al., 1991; Moran et al., 1995; Hempel, 1995) and the Juan de Fuca Ridge (Fisher et al., 1994). Fewer studies have addressed permeability in distal turbidites (e.g., Bryant et al., 1986; Wetzel, 1990), carbonates (e.g., Taylor, 1991), and clays (e.g., Bryant and Bennett, 1988; Bryant et al., 1990).

Bryant and Rack (1990) and Marsters and Christian (1990) measured the hydraulic properties of diatomaceous sediments, which were found to have some rather peculiar properties caused by the very high intragranular porosity of diatom frustules: the porosities of these sediments are high and remain so to considerable depths of burial; shear strengths are anomalously high; and measured permeabilities range from semi-pervious ($2 \times 10^{-13} \text{ m}^2$, comparable to sandstone) to virtually impervious ($4 \times 10^{-18} \text{ m}^2$). Bryant and Rack (1990) demonstrated a high degree of correlation ($R = \sim 0.8$) between porosity and the abundance of diatom frustules in the sediments from the Weddell Sea. They also noted that the samples with the highest permeabilities are rich in diatoms, whereas sediments that contain a lower concentration of diatoms can be essentially impermeable, even though their porosities are $>40\%$.

The diatomaceous sediments from Site 1179 have properties similar to the properties of the sediments from the Weddell Sea. Throughout Unit I, to a depth of nearly 225 meters below seafloor (mbsf), the porosity of the sediments exceeds 80%. Porosities actually increase with depth in the upper part of the unit, reaching a maximum of $\sim 86\%$ at 140 mbsf; there is a corresponding decrease of grain density to a minimum near 2200 kg/m^3 . Because siliceous microfossils are composed of opaline silica with a density $<2100 \text{ kg/m}^3$, we suspect that these trends are related to the abundance of diatoms and that permeability is similarly affected.

The discovery of deep microbial activity (the "deep biosphere") provides a new impetus to measure sediment permeabilities. As noted previously, one of the objectives of drilling at Site 1179 was to search for microbes and/or chemical evidence of biological activity in the sediments as part of the ongoing effort to discover the depth and lateral extent of the deep biosphere. Two lines of evidence that may prove to be indicative of ongoing microbial activity in the sediment column at Site 1179 are observed variations of ammonia and sulfate concentrations with depth. Transport properties of diffusion, advection, and permeability are important to the search for deep biological activity. Chemical profiles that may provide indirect evidence of microbial activity are affected by advection and diffusion. Diffusion, the movement of ions and molecules down concentration gradients, depends on the diffusion coefficient, which is a material property of porous media. Advection, the physical movement of pore water driven by pressure gradients, depends on permeability, which is also a material property. Diffusion coeffi-

coefficients are approximately proportional to permeability because both diffusion and fluid flow depend on the connectivity of the pore spaces; a permeability of 10^{-12} m^2 (1 nd) is roughly equivalent to the diffusion coefficient for salts in aqueous solution (Brace et al., 1968). Whether diffusion or advection is the dominant process depends on the pressure gradient. Where rates of advection and diffusion are very low, pore water chemistry profiles may be “fossils” that change little, even over geologic time. Conversely, high rates of either flow or diffusion cause mixing of the pore water; under these conditions, significant chemical gradients must be maintained by dynamic chemical processes such as microbial activity. Another consideration is that some degree of permeability is required to support life in the deep biosphere. Living organisms cannot persist at depth unless there are sufficient fluxes of nutrients, waste products, and microbes themselves through the sediments. Permeability is thus a measure of the viability of the sediment as a habitat for bacteria; impervious sediments are unlikely habitats for microbes.

MATERIALS AND METHODS

Experimental Method

Sediment permeability is most commonly measured by one of three methods (Bryant et al., 1975, 1981). Falling-head permeameters are accurate only when permeabilities are high. Constant-head permeameters are in common use but are difficult to use for fine-grained materials. Most measurements made on deep-sea sediments have been made by oedometer compaction tests, in part because high backpressures can be used to ensure complete water saturation. However, oedometer tests suffer from significant systematic errors when sample diameters are smaller than several inches (Olson, 1986). A fourth method for measuring permeabilities in “tight” materials such as crystalline rocks and shales is the transient-pulse test (TPT) pioneered by Brace et al. (1968) and refined by Sutherland and Cave (1980) and Trimmer (1981). A schematic diagram of the experimental apparatus is shown in Figure F1.

Briefly, the transient-pulse method consists of placing a cylindrical sample between two pore-fluid reservoirs at equal pressure. The pressure on the “upstream” side is increased by an increment, ΔP . The pressure difference between the upstream and downstream reservoirs ($P_u - P_d$, respectively) is then recorded for a suitable period of time as it decays toward a new equilibrium value, P_f . The time-dependent pressure decay depends on the permeability of the sample:

$$P_u - P_d = \Delta p e^{-\alpha t}, \quad (1)$$

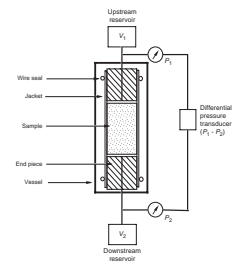
where

$$\alpha = (kA/\mu\beta L)[(1/V_u) + (1/V_d)], \quad (2)$$

and

- k = material permeability,
- μ = fluid viscosity,
- β = fluid compressibility,
- A = sample cross-sectional area,

F1. Transient-pulse technique apparatus, p. 10.



L = sample length,
 V_u = upstream reservoir volume, and
 V_d = downstream reservoir volume.

α is found by linear regression from

$$\ln(P_u - P_d) = \ln(\Delta p) - \alpha t, \quad (3)$$

and the permeability is given by

$$k = \alpha(\mu\beta L/A)[(1/V_u) + (1/V_d)]^{-1}. \quad (4)$$

TPT has been used to measure permeabilities as low as $5 \times 10^{-21} \text{ m}^2$ in Wilcox shale with a precision of 1%–3%; sample-to-sample variability is ~10% (Kwon et al., 2001).

Samples

As shown in Figure F2, sediments from three sedimentary units were recovered at Site 1179 (Kanazawa, Sager, Escutia, et al., 2001):

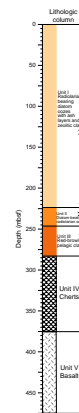
- Unit I (0–223.5 mbsf) is a radiolarian-bearing diatom ooze, composed of diatoms (40%–60%), radiolarians (10%–35%), and clay (illite) with small amounts of quartz. The dominant particle size is silt.
- Unit II (223.5–246.0 mbsf) is a clay- and diatom-rich radiolarian ooze. The dominant constituents are radiolarians (40%–60%), diatom frustules (13%–17%), and clays (20%–35%).
- Unit III (246.0–283.5 mbsf) is composed of brown pelagic clay (clay content = 75%–99%). The clays are typically aggregates cemented by zeolites. Unit III contains little, if any, biogenic material.

Sample Preparation

Twenty samples were collected from the sediment column at Site 1179 for permeability studies. The sample set includes 17 samples from Unit I, 2 samples from Unit II, and 1 sample from Unit III. The samples are half rounds with a diameter of ~6.5 cm and a thickness of 5 cm. On the ship, the samples were packed wet, wrapped in foil, and then coated with wax and placed in refrigerated storage. They were shipped in a refrigerated van to the Gulf Coast core repository at the Ocean Drilling Program (ODP) at Texas A&M University in College Station, Texas. They remained in refrigerated storage until the permeability measurements were made. We chose six of these samples for the permeability measurements: four from Unit I, one from Unit II, and one from Unit III.

Samples were prepared for the permeability measurements by using a standard cork punch to cut a core 1.9 cm in diameter and trimming the ends to form right circular cylinders ~2 cm long. The samples were then immersed in salt water under vacuum for 2 days to ensure that they were water saturated. For the TPT measurements, porous stones were placed between the ends of the sample cylinder and a pair of pistons with axial pore pressure ports, and the entire assembly was jacketed with a heat-shrinkable polyolefin tube, as shown in Figure F1. A seal between the jacket and the pistons was achieved by tying Nychrome wires over grooves in the pistons.

F2. Site 1179 lithostratigraphy, p. 11.



After the permeability measurements were completed, the samples were sent to Core Labs, Inc., for laser grain size analysis. Measurements of bulk density, grain density, and porosity were made on samples from adjacent parts of the core.

Permeability Measurements

We found that the procedure was quite sensitive to the effects of small variations of temperature, which affect reservoir volumes and, hence, pressures. The source of the problem proved to be air circulation in the laboratory. We insulated the apparatus by packing the instrument housing with crumpled paper and draping the entire apparatus with a polyethylene sheet. We further reduced the influence of temperature variations on the measurements by limiting the duration of each test.

Sample permeabilities were measured by first increasing the confining pressure and pore pressure in small increments (to avoid deforming the sample) to a differential pressure that approximates the in situ conditions for the sample. Then the pressure in the upstream reservoir was raised by a few kiloPascal (kPa) (typically ~15% of the confining pressure), and the differential pressure between the upstream and downstream reservoirs ($P_u - P_d$) was recorded using a Validyne differential pressure transducer until the differential pressure decayed to 20%–30% of its initial value. The permeability of each sample was then estimated by fitting equation 3 to the data, to determine α , and then calculating k from equation 4, as described above.

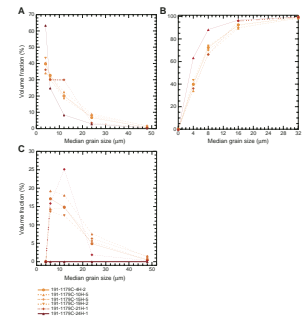
RESULTS

The grain size distributions are summarized in Figure F3. Grain sizes range from <4 to 50 μm , and the range of mean sample grain sizes is 3 to 6 μm . In all of these samples, abundance of grains of a particular size decreases with increasing grain size. The grain size distributions for the four samples from Unit I are very similar. By contrast, the clay from Unit III is dominated by grain sizes <8 μm . The diatom-bearing radiolarian ooze from Unit II has a grain size distribution intermediate between Unit I and Unit III in that the abundance of very small grains is comparable to that of Unit I, whereas the abundance of larger grains is comparable to Unit III. However, this sample is enriched in 12- μm grains relative to both the overlying diatom ooze and the underlying clay. Figure F3C shows the grain size distribution relative to the Unit III clay. Here we have assumed that the clay is a background material; then we calculated the fractions of coarser grain sizes that must be added to the clay to obtain the observed grain size distributions of the other five samples. Figure F3C indicates that the biogenic oozes (Units I and II) are enriched in grain sizes between 4 and 24 μm relative to the underlying pelagic clay.

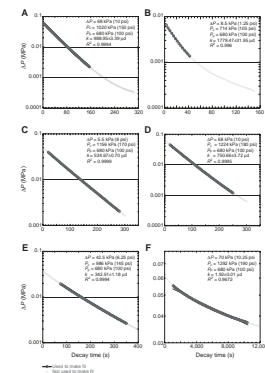
The permeability data are shown in Figure F4 and are summarized in Table T1.

A first point worthy of note is that our data (Fig. F4) suggest that the permeabilities of these samples vary with effective pressure, as evidenced by the fact that the plots of $\ln(P_u - P_d)$ vs. time are not linear; k decreases as the pressure pulse decays. This behavior is a consequence of the fact that permeability depends on the effective cross section or aperture of the channels in the rock, which in turn depend on the effec-

F3. Grain size distributions, p. 12.



F4. Pressure differences vs. time, p. 13.



T1. Sample permeabilities and bulk properties, Site 1179, p. 16.

tive or applied pressure (e.g., Gangi, 1978). As effective pressure increases, void spaces are compressed and apertures decrease, leading to lower permeabilities. Based on an asperity deformation model, Gangi (1978) has shown that for media containing cracks,

$$k \approx k_0[1 - (P_e/P_1)^m], \quad (5)$$

where k_0 is the permeability of the medium at $P_e = 0$, P_1 is a modulus term for the asperities, and m describes the power-law distribution of asperity heights. A fit of this model by Gangi (1978) to experimental data obtained by Nelson (1975), shown in Figure F5, serves to illustrate the effect.

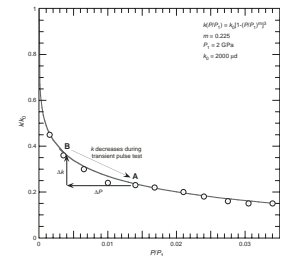
In our experiments, we first apply approximate in situ effective pressure (A in Fig. F5) and then an additional increment of pressure, ΔP , is added to the upstream reservoir. Thus, at $t = 0$, the effective pressure at the upstream end of the sample is $P_e = P_c - P_p - \Delta P$ (B in Fig. F5). Hence, the pressure increment has the effect of decreasing the effective pressure and increasing the permeability of the sample by an amount Δk at the initiation of the test. Subsequently, as the pulse decays, the effective pressure increases, leading to the observed progressive decrease in permeability. Moreover, the highest variation of permeability with effective pressure occurs at low effective pressures. Hence, our samples exhibit this behavior particularly well because the measurements were made at low effective pressures. A complete analysis of this behavior using the transient-pulse method is beyond the scope of this paper. Consequently, our estimates of permeability are based on fits to linear portions of the decay curves shown in Figure F4.

Estimated permeabilities of the diatom oozes from Unit I range from 534 to 1604 μd , whereas the permeability of the radiolarian ooze from Unit II is slightly lower (289 μd) and the permeability of the Unit III pelagic clay is two orders of magnitude lower ($\sim 1.9 \mu\text{d}$) (see Table T1).

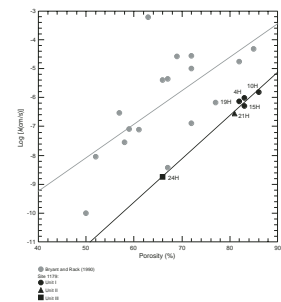
Figure F6 is a plot of $\log(k)$ vs. porosity for our samples. Also shown are the data for diatomaceous sediments from the Weddell Sea (Bryant and Rack, 1990). Although there is a clear correlation between $\log(k)$ and ϕ ($R = 0.99$), the relationship is not necessarily linear because the data from Units I and II lie in a cluster. The data for samples from Units I and II alone lie on a similar trend, but the correlation is lower ($R = 0.87$) and significant at the 0.06 level but not at the 0.05 level.

While the effect is difficult to quantify from the available data, there is also an apparent relationship between permeability and grain size among our samples. Figure F3C suggests that the sample with the highest proportion of coarser grain sizes (from Core 191-1179C-10H) also has the highest permeability, followed in order by the samples from Cores 15H, 19H, 4H, 21H (Unit II), and 24H (Unit III). Although they lie on a similar trend, our samples have appreciably lower permeabilities than the samples from the Weddell Sea, relative to their porosities. The reason for this difference is probably related to the diatom contents of the sediments. The sediments from Unit I at Site 1179 contain 40%–60% diatoms, whereas all of the samples from the Weddell Sea with porosities $>75\%$ contain more than 80% diatoms (Bryant and Rack, 1990).

F5. Permeability with pressure variations, p. 14.



F6. Permeability vs. porosity, p. 15.



ACKNOWLEDGMENTS

This research used samples and data provided by the Ocean Drilling Program (ODP). ODP is sponsored by the U.S. National Science Foundation (NSF) and participating countries under management of Joint Oceanographic Institutions (JOI), Inc. Funding for this research was provided by a grant from the U.S. Science Support Program. We thank Brann Johnson for the use of his laboratory facilities. We also thank the captain and crew of the *JOIDES Resolution*. We are particularly indebted to ODP and ODP technicians Anastasia Ledwon and Jessica Huckemeyer.

REFERENCES

- Brace, W.F., Walsh, J.B., and Frangos, W.T., 1968. Permeability of granite under high pressure. *J. Geophys. Res.*, 80:2225–2236.
- Bryant, W.R., Bennett, R.H., and Katherman, C.E., 1981. Shear strength, consolidation, porosity, and permeability of oceanic sediments. In Emiliani, C. (Ed.), *The Sea* (Vol. 7): *The Oceanic Lithosphere*: New York (Wiley), 1555–1616.
- Bryant, W., Wetzel, A., Taylor, E., and Sweet, W., 1986. Consolidation characteristics and permeability of Mississippi Fan sediments. In Bouma, A.H., Coleman, J.M., Meyer, A.W., et al., *Init. Repts. DSDP*, 96: Washington (U.S. Govt. Printing Office), 797–809.
- Bryant, W.R., and Bennett, R.H., 1988. Origin, physical and mineralogical nature of red clays: the Pacific Ocean as a model. *Geo-Mar. Lett.*, 8:189–249.
- Bryant, W.R., Bennett, R.H., Burkett, P.J., and Rack, F.R., 1990. The fabric of a consolidating clayey sediment column, ODP Site 697. In Barker, P.F., Kennett, J.P., et al., *Proc. ODP, Sci. Results*, 113: College Station, TX (Ocean Drilling Program), 225–237.
- Bryant, W.R., Hottman, W., and Trabant, P., 1975. Permeability of unconsolidated and consolidated marine sediments, Gulf of Mexico. *Mar. Geotechnol.*, 1:1–14.
- Bryant, W.R., and Rack, F.R., 1990. Consolidation characteristics of Weddell Sea sediments: results of ODP Leg 113. In Barker, P.F., Kennett, J.P., et al., *Proc. ODP, Sci. Results*, 113: College Station, TX (Ocean Drilling Program), 211–223.
- Fisher, A.T., Fischer, K., Lavoie, D., Langseth, M., and Xu, J., 1994. Geotechnical and hydrogeological properties of sediments from Middle Valley, northern Juan de Fuca Ridge. In Mottl, M.J., Davis, E.E., Fisher, A.T., and Slack, J.F. (Eds.), *Proc. ODP, Sci. Results*, 139: College Station, TX (Ocean Drilling Program), 627–647.
- Gangi, A.F., 1978. Variation of whole and fractured rock permeability with confining pressure. *Int. J. Rock Mech. Min. Sci.*, 15:249–257.
- Hempel, P., 1995. Dewatering of sediments along the Cascadia margin: evidence from geotechnical properties. In Carson, B., Westbrook, G.K., Musgrave, R.J., and Suess, E. (Eds.), *Proc. ODP, Sci. Results*, 146 (Pt. 1): College Station, TX (Ocean Drilling Program), 257–274.
- Kanazawa, T., Sager, W.W., Escutia, C., et al., 2001. *Proc. ODP, Init. Repts.*, 191 [CD-ROM]. Available from: Ocean Drilling Program, Texas A&M University, College Station TX 77845-9547, USA.
- Kwon, O., Kronenberg, A.K., Gangi, A.F., and Johnson, B., 2001. Permeability of Wilcox shale and its effective pressure law. *J. Geophys. Res.*, 106:19339–19353.
- Marsters, J.C., and Christian, H.A., 1990. Hydraulic conductivity of diatomaceous sediment from the Peru continental margin obtained during ODP Leg 112. In Suess, E., von Huene, R., et al., *Proc. ODP, Sci. Results*, 112: College Station, TX (Ocean Drilling Program), 633–638.
- Moran, K., and Christian, H.A., 1990. Strength and deformation behavior of sediment from the Lesser Antilles forearc accretionary prism. In Moore, J.C., Mascle, A., et al., *Proc. ODP, Sci. Results*, 110: College Station, TX (Ocean Drilling Program), 279–288.
- Moran, K., Gray, W.G.D., and Jarrett, C.A., 1995. Permeability and stress history of sediment from the Cascadia margin. In Carson, B., Westbrook, G.K., Musgrave, R.J., and Suess, E. (Eds.), *Proc. ODP, Sci. Results*, 146 (Pt. 1): College Station, TX (Ocean Drilling Program), 275–280.
- Nelson, R., 1975. Fracture permeability in porous reservoirs: experimental and field approach [Ph.D. dissert.]. Texas A&M Univ., College Station, TX.
- Olson, R.E., 1986. State of the art: consolidation testing. In Young, R.N., and Townsend, F.C. (Eds.), *Consolidation of Soils: Testing and Evaluation*. ASTM Spec. Tech. Publ., 892:7–70.
- Sutherland, H.J., and Cave, S.P., 1980. Argon gas permeability of New Mexico rock salt under hydrostatic compression. *Int. J. Rock Mech. Min. Sci.*, 17:281–288.

- Taylor, E., 1991. Physical properties and consolidation of the calcareous sediments of Broken and Ninetyeast Ridges. *In* Weissel, J., Peirce, J., Taylor, E., Alt, J., et al., *Proc. ODP, Sci. Results*, 121: College Station, TX (Ocean Drilling Program), 253–260.
- Taylor, E., Burkett, P.J., Wackler, J.D., and Leonard, J.N., 1991. Physical properties and microstructural response of sediments to accretion-subduction: Barbados forearc. *In* Bennett, R.H., Bryant, W.R., and Hulbert, M.H. (Eds.), *Microstructure of Fine-Grained Sediments: from Mud to Shale*: New York (Springer), 213–228.
- Trimmer, D.A., 1981. Design criteria for laboratory measurements of low permeability rocks. *Geophys. Res. Lett.*, 8:973–975.
- Wetzel, A., 1990. Consolidation characteristics and permeability of Bengal Fan sediments drilled during Leg 116. *In* Cochran, J.R., Stow, D.A.V., et al., *Proc. ODP, Sci. Results*, 116: College Station, TX (Ocean Drilling Program), 363–368.

Figure F1. Schematic diagram of experimental apparatus for the transient-pulse technique for measuring permeability at elevated pressures.

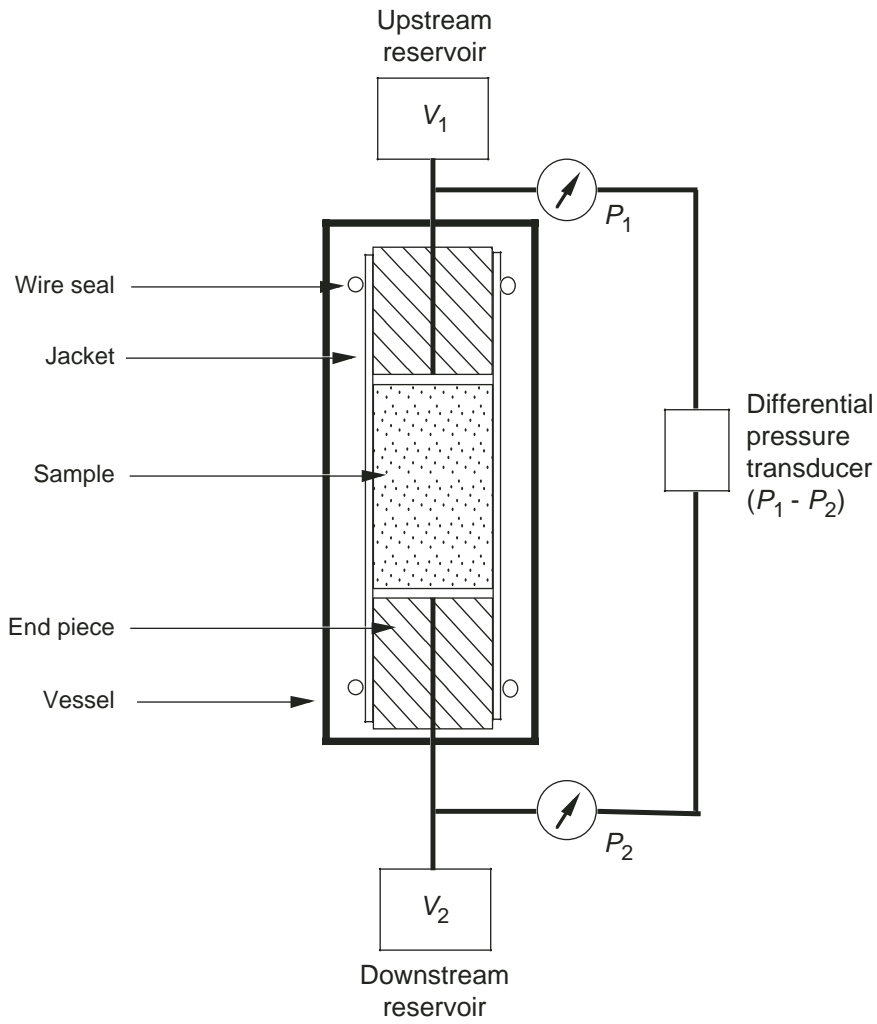


Figure F2. Lithostratigraphy at ODP Site 1179. Arrows = locations of permeability samples.

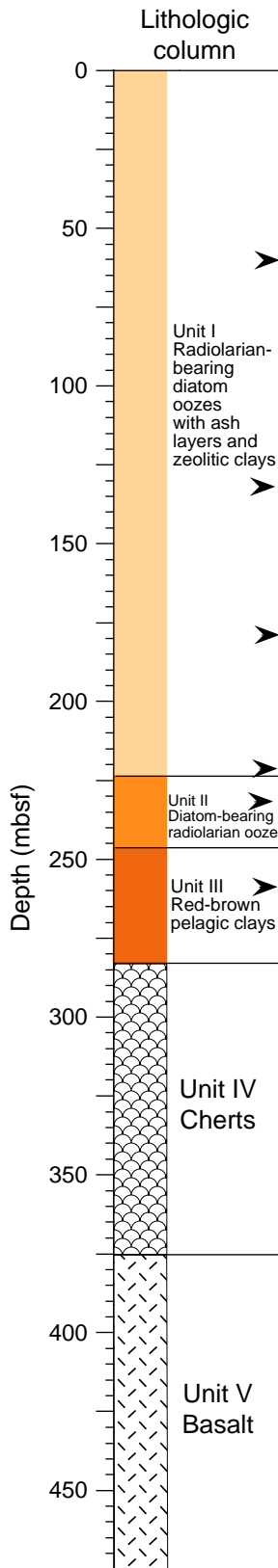


Figure F3. A–C. Grain size distributions in permeability samples from Site 1179.

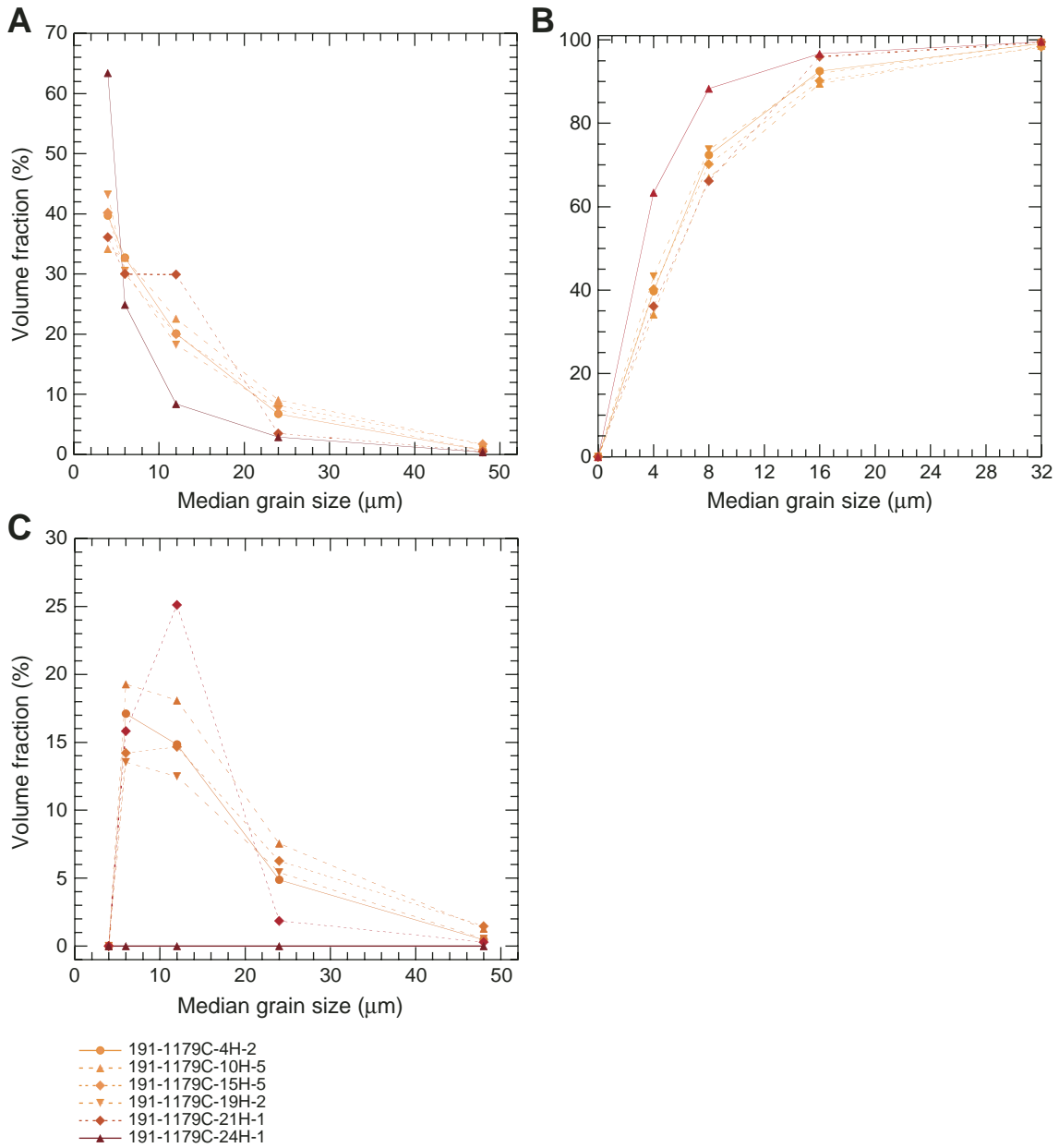


Figure F4. Pressure difference between the upstream and downstream reservoirs ($P_u - P_d$) vs. time for each of the six samples included in this study. Red symbols = data used to estimate the permeability of the sample, solid line = best fit. **A.** Sample 191-1179C-4H-2, 145–150 cm. **B.** Sample 191-1179C-10H-5, 145–150 cm. **C.** Sample 191-1179C-15H-5, 145–150 cm. **D.** Sample 191-1179C-19H-2, 145–150 cm. **E.** Sample 191-1179C-21H-1, 145–150 cm. **F.** Sample 191-1179C-24H-1, 145–150 cm.

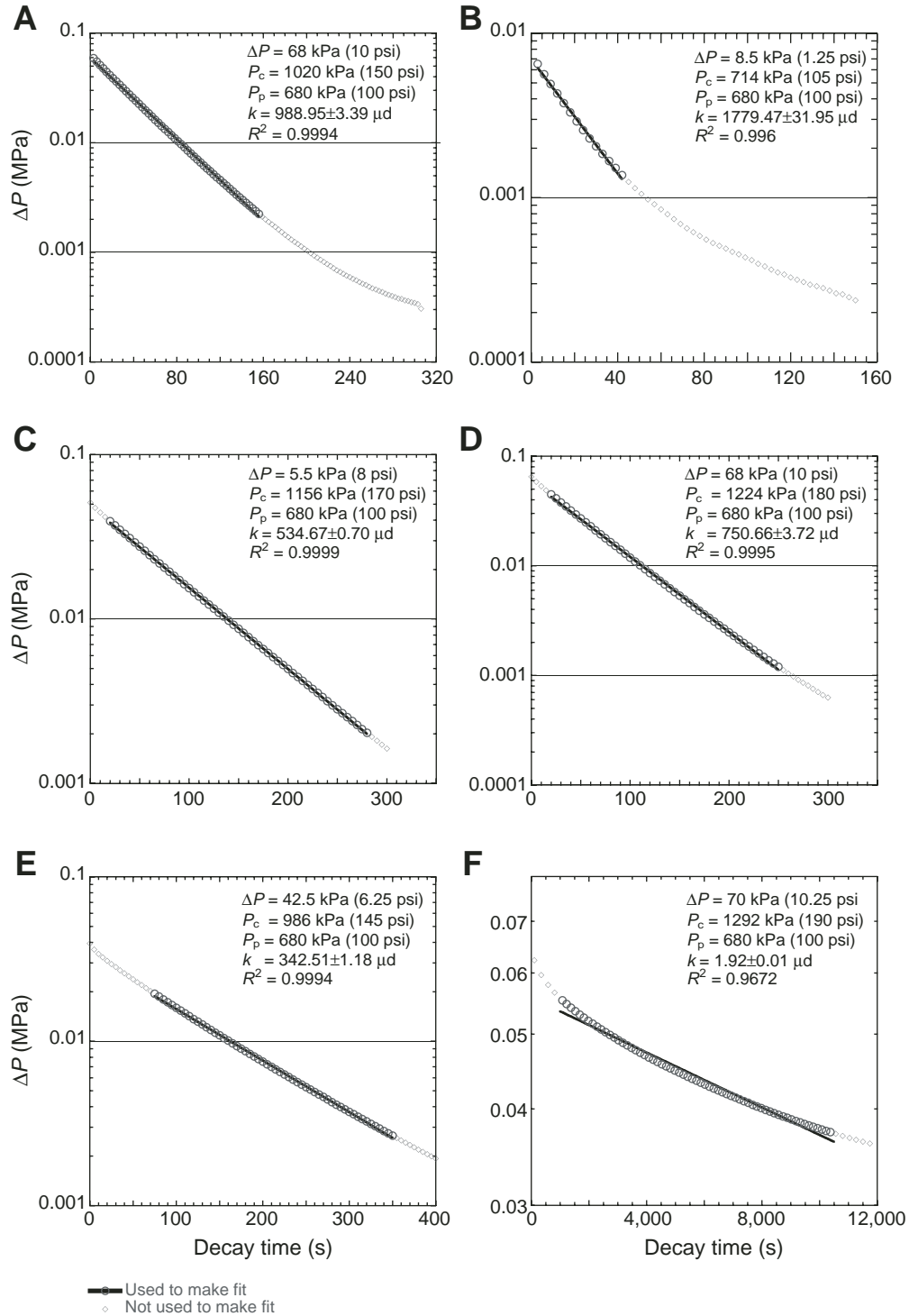


Figure F5. Variation of permeability with pressure in Navajo Sandstone (modified from Gangi, 1978; data from Nelson, 1975).

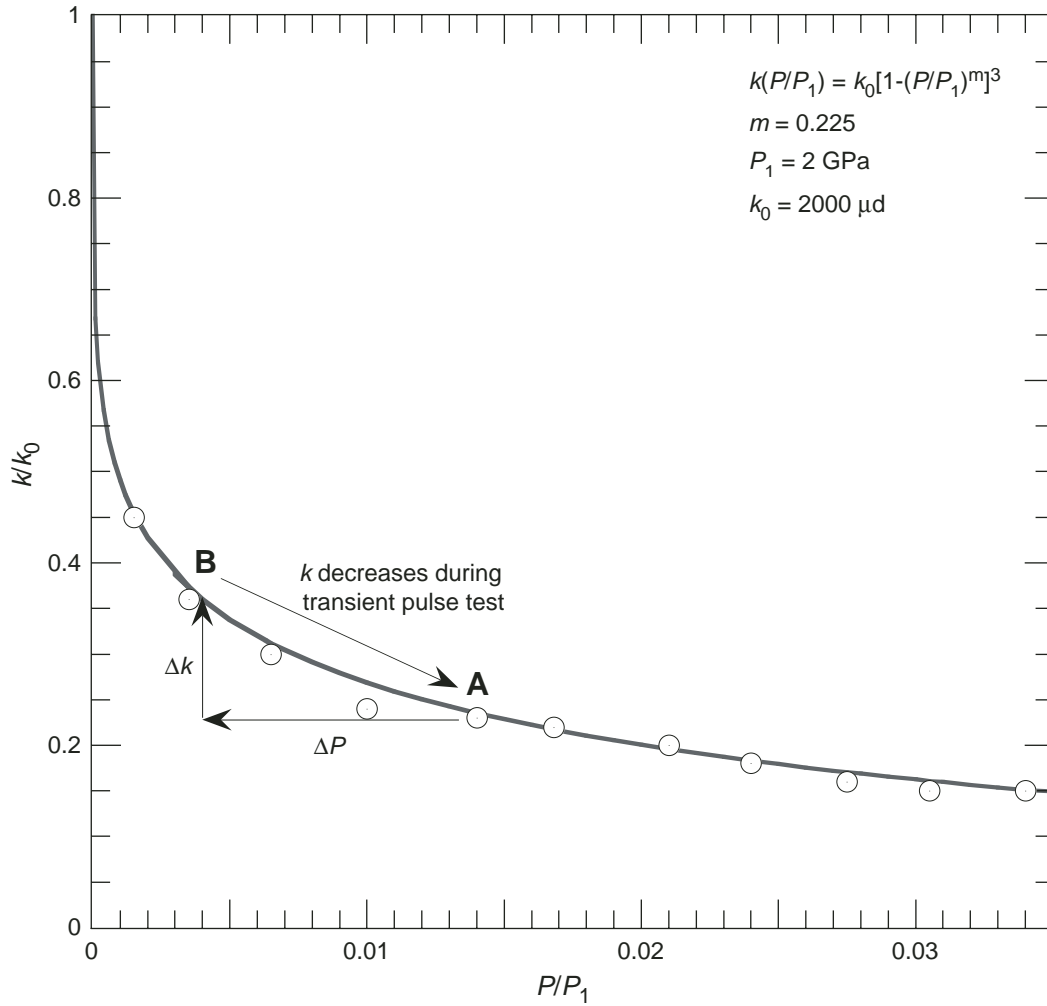


Figure F6. Permeability vs. porosity in diatomaceous sediments from the Weddell Sea, ODP Leg 113 (Bryant and Rack, 1990), and samples from Site 1179 (core numbers are indicated).

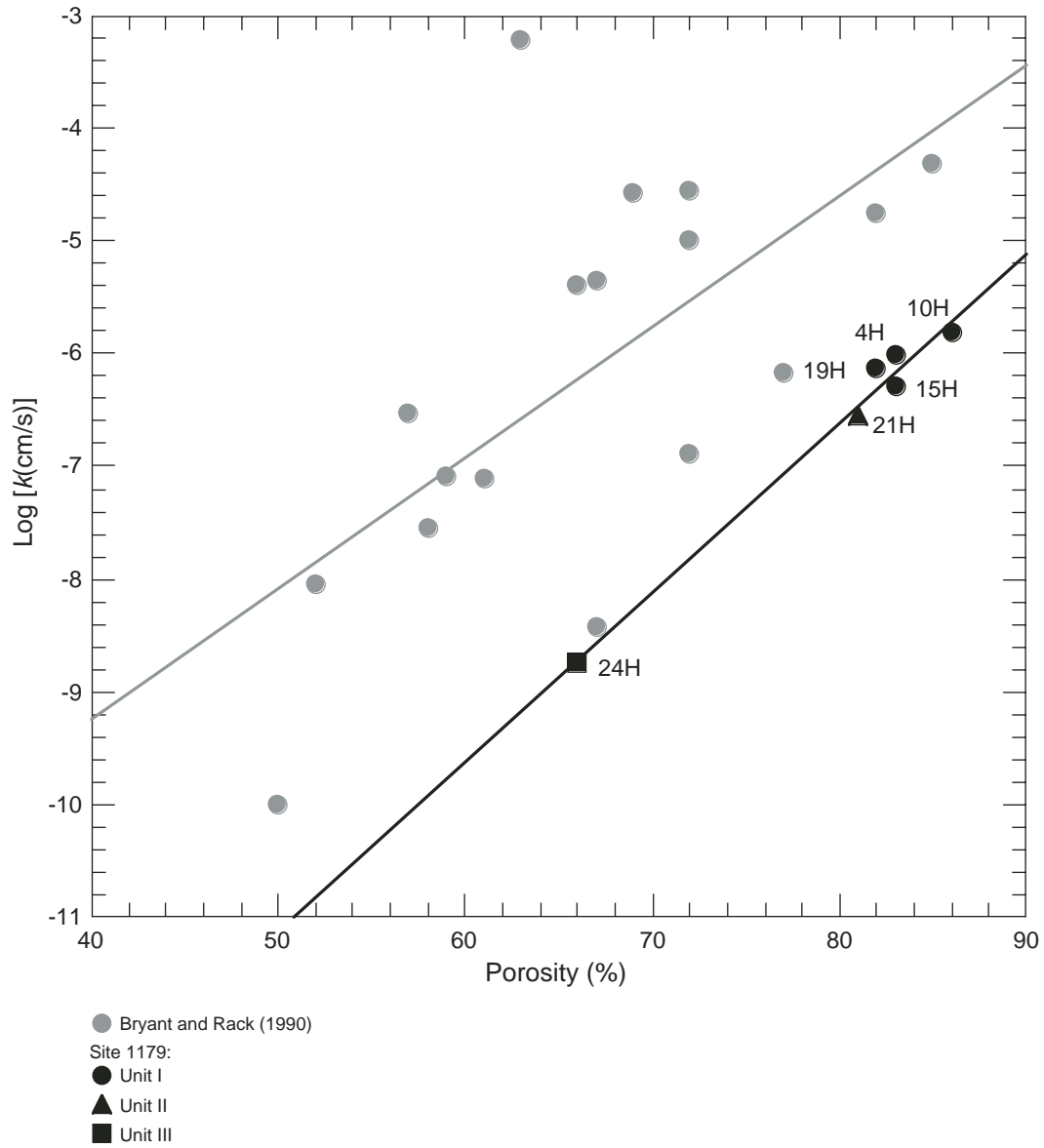


Table T1. Summary of permeabilities and bulk properties of samples, Site 1179.

Core, section, interval (cm)	Unit	Depth (mbsf)	Density (kg/m ³)	Grain size (μ m)	Porosity (%)	Permeability (μ d)	Conductivity (cm/s $\times 10^{-9}$)	P_c (kPa)	P_e (kPa)	ΔP (kPa)
191-1179C-										
4H-2, 145-150	I	70.3	1.3	6	83	999.0 \pm 3.4	965.0 \pm 3.3	1020	340	68
10H-5, 145-150	I	131.8	1.2	6	86	1604.2 \pm 9.5	1549.7 \pm 9.2	714	34	8.5
15H-5, 145-150	I	179.3	1.3	6	83	534.7 \pm 0.7	516.5 \pm 0.7	1156	476	55
19H-2, 145-150	I	121.8	1.3	5	82	750.7 \pm 3.7	725.2 \pm 3.6	1224	544	68
21H-1, 145-150	II	230.3	1.3	6	81	288.6 \pm 0.7	278.8 \pm 0.7	986	306	42.5
24H-1, 145-150	III	259.0	1.5	3	66	1.92 \pm 0.01	1.85 \pm 0.01	1292	612	70